Weak second order explicit stabilized methods for stiff stochastic differential equations

Assyr Abdulle[1], Gilles Vilmart[2], and Konstantinos C. Zygalakis[3]

January 14, 2013

Abstract

We introduce a new family of explicit integrators for stiff Itô stochastic differential equations (SDEs) of weak order two. These numerical methods belong to the class of one-step stabilized methods with extended stability domains and do not suffer from the stepsize reduction faced by standard explicit methods. The family is based on the standard second order orthogonal Runge-Kutta Chebyshev methods (ROCK2) for deterministic problems. The convergence, mean-square and asymptotic stability properties of the methods are analyzed. Numerical experiments, including applications to nonlinear SDEs and parabolic stochastic partial differential equations are presented and confirm the theoretical results.

Keywords: Stiff SDEs, explicit stochastic methods, stabilized methods, orthogonal Runge-Kutta Chebyshev, S-ROCK.

AMS subject classification (2010): 65C30, 60H35, 65L20

1 Introduction

We consider stiff systems of Itô stochastic differential equations for which standard explicit integrators – e.g., the well-known Euler-Maruyama method – face a sever step size restriction [15, 13, 17]. Such problems are usually solved numerically by (semi)-implicit methods, which can be expensive for large systems and difficult to implement for complex problems. Recently, a new class of explicit stabilized methods called S-ROCK has been introduced for stiff problems [2, 4]. On the one hand, these methods (fully explicit) are as easy to implement as the Euler-Maruyama method. On the other hand, their extended mean-square stability regions [15] (for suitable test problems) make them much more efficient than classical explicit methods for stiff problems.

In this paper, we introduce a weak second order family of explicit stabilized integrators based on the second order ROCK2 integrators for deterministic stiff problems. The main feature of the algorithm is that it has an arbitrarily large mean-square stability region that grows quadratically with respect to the number of drift function evaluations. For an efficient implementation, the integrators are derivative free, and the number of diffusion function evaluations is independent of the number of Weiner processes involved, similarly to the methods introduced in [31] . As an additional feature, the proposed methods have a large asymptotic stability region close to the origin.

Up to now, with the exception of [19], only weak first order explicit stabilized methods have been proposed for stiff stochastic problems. In [19] an attempt to generalize the S-ROCK methods

[1]Mathematics Section, École Polytechnique Fédérale de Lausanne, Station 8, 1015 Lausanne, Switzerland, Assyr.Abdulle@epfl.ch

[2]École Normale Supérieure de Cachan, Antenne de Bretagne, INRIA Rennes, IRMAR, CNRS, UEB, av. Robert Schuman, F-35170 Bruz, France, Gilles.Vilmart@bretagne.ens-cachan.fr

[3]School of Mathematics, University of Southampton, Southampton SO17 1BJ, UK, k.zygalakis@soton.ac.uk

to weak second order has been proposed. However, this generalization involves the solution of a large number of order conditions and the resulting methods have less favorable mean-square stability properties than the methods proposed in this paper (see e.g., [2, 4]).

This paper is organized as follows. We recall in Section 2 the concept of stabilized methods for stiff SDEs. In Section 3, we introduce our new weak second order explicit stabilized integrators and analyze their weak order of convergence and stability properties. Finally, we present in Section 4 various numerical experiments, both for linear and non-linear stiff SDEs and for a parabolic stochastic partial differential equation (SPDE), that illustrate the efficiency of the proposed methods.

2 Stabilized stochastic methods

We briefly recall the notions of weak convergence, mean-square and asymptotic stabilities.

2.1 Weak stochastic integrators

We consider the Itô stochastic system of differential equations

$$dX(t) = f(X(t))dt + \sum_{r=1}^{m} g^r(X(t))dW_r(t), \quad X(0) = X_0, \tag{1}$$

where $X(t)$ is a random variable with values in $\mathbb{R}^N$, $f : \mathbb{R}^N \to \mathbb{R}^N$ is the drift term, $g^r : \mathbb{R}^N \to \mathbb{R}^N$, $r = 1, \ldots, m$ are the diffusion terms, and $W_r(t)$, $r = 1, \ldots, m$ are independent one-dimensional Weiner processes. The drift and diffusion functions are assumed smooth enough, Lipschitz continuous and to satisfy a growth bound in order to ensure a unique (mean-square bounded) solution of (1) [7, 17]. For the numerical approximation of (1) we consider the discrete map

$$X_{n+1} = \Psi(X_n, h, \xi_n), \tag{2}$$

where $\Psi(\cdot, h, \xi_n) : \mathbb{R}^N \to \mathbb{R}^N$, $X_n \in \mathbb{R}^N$ for $n \geq 0$, h denotes the timestep size, and ξ_n denotes a random vector. The numerical approximation (2), starting from the exact initial condition X_0 of (1) is said to have weak order τ if for all functions[1] $\phi : \mathbb{R}^N \to \mathbb{R} \in C_P^{2(\tau+1)}(\mathbb{R}^N, \mathbb{R})$,

$$|\mathbb{E}(\phi(X_n)) - \mathbb{E}(\phi(X(t_n)))| \leq Ch^\tau, \tag{3}$$

and to have strong order τ if

$$\mathbb{E}(|X_n - X(t_n)|) \leq Ch^\tau, \tag{4}$$

for any $t_n = nh \in [0, T]$ with $T > 0$ fixed, for all h small enough, with constants C independent of h.

Remark 2.1. *A well-known theorem of Milstein [25] (see [27, Chap. 2.2]) allows to infer the global weak order from the error after one step. Assuming that $f, g^r \in C_P^{2(\tau+1)}(\mathbb{R}^N, \mathbb{R}^N), r = 1, \ldots, m$ are Lipschitz continuous, that for all $r \in \mathbb{N}$, the moments $\mathbb{E}(|X_n|^{2r})$ are bounded for all n, h with $0 \leq nh \leq T$ uniformly with respect to all h sufficiently small, and that the local error bound for all $\phi \in C_P^{2(\tau+1)}(\mathbb{R}^N, \mathbb{R})$ and all initial values $X(0) = X_0$ satisfies*

$$|\mathbb{E}(\phi(X_1)) - \mathbb{E}(\phi(X(t_1)))| \leq Ch^{\tau+1} \tag{5}$$

[1] Here and in what follows, $C_P^\ell(\mathbb{R}^N, \mathbb{R})$ denotes the space of ℓ times continuously differentiable functions $\mathbb{R}^N \to \mathbb{R}$ with all partial derivatives with polynomial growth.

for all h sufficiently small, then the global error bound (3) *holds. Here the constant C is again independent of h. For the strong convergence we have the following result [26]. If the functions f, g^r are sufficiently smooth and Lipschitz continuous and*

$$\mathbb{E}|X_1 - X(t_1)| \le Ch^{\tau+1/2} \quad \textit{and} \quad |\mathbb{E}(X_1) - \mathbb{E}(X(t_1))| \le Ch^{\tau+1}, \tag{6}$$

for all initial values $X(0) = X_0$, then the global error bound (4) *holds.*

The simplest method to approximate solutions to (1) is the so-called Euler-Maruyama method

$$X_{n+1} = X_n + hf(X_n) + \sum_{r=1}^{m} g^r(X_n)\Delta W_{n,r}, \tag{7}$$

where $\Delta W_{n,r} \sim \mathcal{N}(0,h),\ r = 1,\dots m$ are independent Weiner increments. This method has strong order $1/2$ and weak order 1 for a general system of Itô SDEs [23]. Various higher order weak methods have been considered in the literature [17, 27]. For example, weak second order methods were proposed by Milstein [24, 25], Platen [28], Talay [34] and Tocino and Vigo-Aguiar [37], and more recently Runge-Kutta type methods of Rößler [30]. We mention also the extrapolation methods of Talay and Tubaro [35] and of [18] that combines methods with different stepsizes to achieve higher weak order convergence. In [3], (semi)-implicit weak second order methods with favorable geometric and/or stability properties were introduced using the framework of modified differential equations. This framework could in principle be used to construct higher order weak stabilized methods. Here we follow a different approach based on stabilizing a second weak order scheme originating from the weak second order Taylor method known as the Milstein-Talay method [34]

$$\begin{aligned} X_1 &= X_0 + hf(X_0) + \sum_{r=1}^{m} g^r(X_0)\Delta W_r + \sum_{q,r=1}^{m} (g^r)'(X_0)g^q(X_0)I_{q,r} \\ &+ \frac{h^2}{2}\Big(f'(X_0)f(X_0) + \frac{1}{2}\sum_{r=1}^{m} f''(X_0)(g^r(X_0), g^r(X_0))\Big) + \sum_{r=1}^{m} f'(X_0)g^r(X_0)I_{r,0} \\ &+ \sum_{r=1}^{m}\Big((g^r)'(X_0)f(X_0) + \sum_{q=1}^{m}\frac{1}{2}(g^r)''(X_0)(g^q(X_0), g^q(X_0))\Big)I_{0,r}, \end{aligned} \tag{8}$$

where $I_{r,0}, I_{0,r}, I_{q,r}$ denote the stochastic integrals defined by

$$I_{r,0} = \int_{t_0}^{t_1}\int_{t_0}^{t} dW_r(s)dt,\ I_{0,r} = \int_{t_0}^{t_1}\int_{t_0}^{t} ds\ dW_r(t),\ I_{q,r} = \int_{t_0}^{t_1}\int_{t_0}^{t} dW_q(s)dW_r(t). \tag{9}$$

Here, we use the notations $f'(X_0)\cdot$ for the first derivative (a linear form) and $f''(X_0)(\cdot,\cdot)$ for the second derivative (a symmetric bilinear form) of f at the point X_0 and similar notations for the diffusion functions g^r. Notice that for notational brevity, we shall always write X_1 and X_0 in place of X_{n+1} and X_n when introducing an integrator. As given above, the method (8) is not practical for implementation: it contains derivatives which are expensive in general, and stochastic integrals that are difficult to simulate. We will discuss these issues in Section 3.1 where we derive a stabilized explicit version of the Milstein-Talay method suitable for stiff problems.

2.2 Stability concepts for SDEs

In practice it is not only the order of convergence that guarantees an efficient approximation of an SDE, but also the long-time behavior of the solution. Stability properties of the exact and the numerical solutions are important to understand this behavior. Widely used characterizations of

stability for SDEs are the mean-square and the asymptotic stability (in the large) [7, 14]. The former measures the stability of moments, the latter measures the overall behavior of sample paths. In particular, we have the following definitions. The steady solution $X \equiv 0$ of (1) with $f(0) = g^r(0) = 0,\ r = 1, \ldots, m$ is called stochastically asymptotically stable in the large if there exists $\delta > 0$ such that

$$\lim_{t\to\infty} |X(t)| = 0 \text{ with probability 1 for all } |X_0| < \delta, \tag{10}$$

mean-square stable if there exists $\delta > 0$, such that

$$\lim_{t\to\infty} \mathbb{E}(|X(t)|^2) = 0 \text{ for all } |X_0| < \delta. \tag{11}$$

2.2.1 The stochastic scalar test equation with multiplicative noise

To gain insight on the stability behavior of a numerical method, we consider a class of linear scalar test problems widely used in the literature [32, 15, 9, 36],

$$dX(t) = \lambda X(t)dt + \mu X(t)dW(t), \qquad X(0) = 1, \tag{12}$$

in dimensions $N = m = 1$, with fixed complex scalar parameters λ, μ. The exact solution of (12), given by $X(t) = \exp((\lambda + \frac{1}{2}\mu^2)t + \mu W(t))$, is stochastically asymptotically stable if and only if $\lim_{t\to\infty} |X(t)| = 0$ with probability 1, equivalently $(\lambda, \mu) \in \mathcal{S}^{AS}_{\mathrm{SDE}}$ with

$$\mathcal{S}^{AS}_{\mathrm{SDE}} := \big\{(\lambda, \mu) \in \mathbb{C}^2 \ ;\ \Re\big(\lambda - \tfrac{1}{2}\mu^2\big) < 0\big\},$$

and mean-square stable if and only if $\lim_{t\to\infty} \mathbb{E}\big(|X(t)|^2\big) = 0$, equivalently $(\lambda, \mu) \in \mathcal{S}^{MS}_{\mathrm{SDE}}$ with

$$\mathcal{S}^{MS}_{\mathrm{SDE}} := \big\{(\lambda, \mu) \in \mathbb{C}^2 \ ;\ \Re(\lambda) + \tfrac{1}{2}|\mu|^2 < 0\big\}.$$

We name the domains $S^{MS}_{\mathrm{SDE}} \subset S^{AS}_{\mathrm{SDE}}$ the mean-square and asymptotic stability domains of the test equation (12), respectively.

Notice that the justification of the test equation (12) is delicate for multi-dimensional systems. Already for multi-dimensional linear systems $dX = AXdt + \sum_{r=1}^m B_r X dW_r(t)$, where A, B_r are $N \times N$ matrices and dW_r are independent one-dimensional Weiner processes, it is difficult to extend the stability analysis of numerical integrators if A and $B_r,\ r = 1, \ldots, m$ do not commute and can thus not be simultaneously diagonalized. This has been investigated in [33, 29] but these studies do not allow for an easy characterization of stability criterion. Using the theory of stochastic stabilization and destabilization [22] an attempt to generalize the linear test equation has been proposed in [8], where two sets of test equations with $N = m = 2$ and $N = m = 3$ have been studied. The conclusion of these studies is that the stability behavior of the Euler-Maruyama method (or its generalization obtained by using the θ method for the drift term) is essentially captured by the test equation (12). We mention however that for linear systems with a non normal drift, the additional test equations in [8] capture stability behaviors (in particular in the pre asymptotic regime) of a numerical scheme that cannot be seen by studying (12). This phenomenon is well known for ODEs (see [13, IV.11]).

2.2.2 Stability of numerical integrators for SDEs

We now look for conditions such that a numerical method (2) applied to the linear test problem (12) yields numerically stable solutions. Similarly to the continuous case we say that the numerical method (2) applied to (12) is said to be

- numerically asymptotically stable if $\lim_{n\to\infty}|X_n| = 0$ with probability 1;
- numerically mean-square stable if $\lim_{n\to\infty}\mathbb{E}(|X_n|^2) = 0$.

Applying a numerical method to the test SDE (12) usually yields [15] the following one step difference equation

$$X_{n+1} = R(p, q, \xi_n)X_n, \tag{13}$$

where $p = \lambda h, q = \mu\sqrt{h}$, and ξ_n is a random variable (e.g. a Gaussian $\xi_n \sim \mathcal{N}(0,1)$ or a discrete random variable). Once this difference equation is formulated, it is not difficult to define the domains of mean-square and asymptotic stability of the numerical method applied to the test SDE (12). In particular, for the numerical mean-square stability, we have [15]

$$\lim_{n\to\infty}\mathbb{E}(|X_n|^2) = 0 \iff (p,q) \in \mathcal{S}^{MS}_{num} \text{ where } \mathcal{S}^{MS}_{num} := \left\{(p,q) \in \mathbb{C}^2 \,; \mathbb{E}|R(p,q,\xi)|^2 < 1\right\}, \tag{14}$$

and for the numerical asymptotic stability, assuming $R(p,q,\xi) \neq 0$ with[2] probability 1 and $\mathbb{E}((\log|R(p,q,\xi)|)^2) < \infty$, it is shown in [15, Lemma 5.1] the equivalence

$$\lim_{n\to\infty}|X_n| = 0 \text{ with probability 1} \iff (p,q) \in \mathcal{S}^{AS}_{num} := \left\{(p,q) \in \mathbb{C}^2 \,;\, \mathbb{E}(\log|R(p,q,\xi)|) < 0\right\}. \tag{15}$$

We denote $\mathcal{S}^{AS}_{num}, \mathcal{S}^{MS}_{num}$, respectively, the above domains of asymptotic and mean-square stability. If we restrict $(p,q) \in \mathbb{R}^2$ then the domains of stability $\mathcal{S}^{AS}_{num} \cap \mathbb{R}^2, \mathcal{S}^{MS}_{num} \cap \mathbb{R}^2$ are called regions of stability.

3 Weak second order explicit stabilized methods

In this section we introduce the S-ROCK2 algorithm for systems of SDEs (1) in the most general setting for non-commutative noise of arbitrary dimension m. The method is obtained by a combination of an efficient weak second order Milstein-Talay scheme with a stabilization procedure based on the second order deterministic stabilized Runge-Kutta method ROCK2.

3.1 Efficient derivative free explicit Milstein-Talay method

We briefly discuss the Milstein-Talay method (8) and explain an efficient implementation of (8) that will be helpful to understand our new S-ROCK2 methods. First it is well-known that one can replace the stochastic integrals $I_{r,0}, I_{0,r}, I_{q,r}$ by discrete random increments without altering the weak order. Consider independent discrete random variables $\chi_r, \xi_r,\ r = 1,\dots,m$ satisfying

$$\mathbb{P}(\chi_r = \pm 1) = 1/2, \quad \mathbb{P}(\xi_r = \pm\sqrt{3}) = 1/6, \quad \mathbb{P}(\xi_r = 0) = 2/3, \tag{16}$$

then both $I_{r,0}$ and $I_{0,r}$ can be replaced by $h^{3/2}\xi_r$ and $I_{q,r}$ can be replaced by

$$J_{q,r} = \begin{cases} h(\xi_r\xi_r - 1)/2 & \text{if } q = r \\ h(\xi_q\xi_r - \chi_q)/2 & \text{if } r < q \\ h(\xi_q\xi_r + \chi_r)/2 & \text{if } r > q. \end{cases} \tag{17}$$

The weak approximation (17) involving $2m-1$ discrete random variables[3] was first proposed in [25] (see also [27, p. 96, eq. (1.25)]). The weak second order method (8) with discrete random

[2] Notice that if $R(p,q,\xi) = 0$ with a non-zero probability, then (13) is clearly numerically asymptotically stable.
[3] Notice that χ_1 is not used in (17) but involved in (21) below.

increments then reads (see e.g. [27, p. 103, eq. (2.18)])

$$\begin{aligned}\hat{X}_1 &= X_0 + hf(X_0) + \sqrt{h}\sum_{r=1}^m g^r(X_0)\xi_r + \sum_{q,r=1}^m (g^r)'(X_0)g^q(X_0)J_{q,r} \\ &+ \frac{h^2}{2}\Big(f'(X_0)f(X_0) + \frac{1}{2}\sum_{r=1}^m f''(X_0)(g^r(X_0), g^r(X_0))\Big) \\ &+ \sum_{r=1}^m \Big((g^r)'(X_0)f(X_0) + \frac{1}{2}\sum_{q=1}^m (g^r)''(X_0)(g^q(X_0), g^q(X_0)) + f'(X_0)g^r(X_0)\Big)\frac{h^{3/2}\xi_r}{2}.\end{aligned} \tag{18}$$

We next briefly discuss derivative free methods. First, using additional Runge-Kutta stages allows to remove $f'f$, $f'g^r$, $f''(g^r, g^r)$ without altering the weak order two of (18),

$$\begin{aligned}K_1 &= X_0 + hf(X_0), \quad K_2 = K_1 + \sqrt{h}\sum_{r=1}^m g^r(X_0)\xi_r, \\ \widetilde{X}_1 &= X_0 + \frac{h}{2}\Big(f(K_2) + f(X_0)\Big) + \sum_{q,r=1}^m (g^r)'(X_0)g^q(X_0)J_{q,r} \\ &+ \sqrt{h}\sum_{r=1}^m \Big(g^r(X_0) + \frac{h}{2}(g^r)'(X_0)f(X_0) + \frac{h}{4}\sum_{q=1}^m (g^r)''(X_0)(g^q(X_0), g^q(X_0))\Big)\xi_r.\end{aligned} \tag{19}$$

Next, we use the following approximation first proposed in [31] to construct efficient derivative free second order methods,

$$\sum_{q,r=1}^m (g^r(X_0))'g^q(X_0)J_{q,r} = \frac{1}{2}\sum_{r=1}^m \Big[g^r\Big(X_0 + \sum_{q=1}^m g^q(X_0)J_{q,r}\Big) - g^r\Big(X_0 - \sum_{q=1}^m g^q(X_0)J_{q,r}\Big)\Big] + \mathcal{O}(h^3). \tag{20}$$

Again, this approximation does not alter the weak second order of the method and requires only 3 evaluations of each function g^r. Notice that in contrast, a naive finite difference approximation e.g., $\frac{1}{2h}\sum_{q,r=1}^m \Big[g^r\Big(x + hg^q(x)\Big) - g^r\Big(x - hg^q(x)\Big)\Big] J_{q,r}$, would require $2m+1$ evaluations of each function g^r at the points $x, x \pm hg^q(x)$. Finally, replacing the last line in (19) by

$$\frac{\sqrt{h}}{2}\sum_{r=1}^m \Big(g^r\big(\frac{X_0 + K_1}{2} + \sqrt{\frac{h}{2}}\sum_{q=1}^m g^q(X_0)\chi_q\big) + g^r\big(\frac{X_0 + K_1}{2} - \sqrt{\frac{h}{2}}\sum_{q=1}^m g^q(X_0)\chi_q\big)\Big)\xi_r, \tag{21}$$

we obtain the scheme

$$\begin{aligned}K_1 &= X_0 + hf(X_0), \quad K_2 = K_1 + \sqrt{h}\sum_{r=1}^m g^r(X_0)\xi_r, \\ \bar{X}_1 &= X_0 + \frac{h}{2}\Big(f(X_0) + f(K_2)\Big) + \frac{1}{2}\sum_{r=1}^m \Big(g^r\Big(X_0 + \sum_{q=1}^m g^q(X_0)J_{q,r}\Big) - g^r\Big(X_0 - \sum_{q=1}^m g^q(X_0)J_{q,r}\Big)\Big) \\ &+ \frac{\sqrt{h}}{2}\sum_{r=1}^m \Big(g^r\big(\frac{X_0 + K_1}{2} + \sqrt{\frac{h}{2}}\sum_{q=1}^m g^q(X_0)\chi_q\big) + g^r\big(\frac{X_0 + K_1}{2} - \sqrt{\frac{h}{2}}\sum_{q=1}^m g^q(X_0)\chi_q\big)\Big)\xi_r.\end{aligned} \tag{22}$$

Each step of the above scheme necessitates only five evaluations of the diffusion functions g^r, $r = 1, \ldots, m$, independently of the dimension m. The method (22) – a modification of the second order method in [17, eq. (2.7) Chap. 14] – seems not to have appeared in the literature, in particular the finite difference discretisation (21) seems new. We give here a direct proof of its weak order two that will be useful in what follows.

Lemma 3.1. *Consider the system of SDEs* (1) *with* $f, g^r \in C_P^6(\mathbb{R}^N, \mathbb{R}^N)$, *Lipschitz continuous. Then the derivative free Milstein-Talay method* (22) *for the approximation of* (1) *satisfies*

$$|\mathbb{E}(\phi(X(nh))) - \mathbb{E}(\phi(\bar{X}_n))| \leq Ch^2, \quad 0 \leq nh \leq T$$

for all $\phi \in C_P^6(\mathbb{R}^N, \mathbb{R})$, *where* C *is independent of* n, h.

Proof. We show that $|\mathbb{E}(\phi(\bar{X}_1)) - \mathbb{E}(\phi(X(t_1)))| \leq Ch^3$ and conclude by Remark 2.1. Since, we already know [34] that $|\mathbb{E}(\phi(\hat{X}_1)) - \mathbb{E}(\phi(X(t_1)))| \leq Ch^3$, where $\hat{X}_1$ is the weak Milstein-Talay method (18), it remains to show that

$$|\mathbb{E}(\phi(\bar{X}_1)) - \mathbb{E}(\phi(\hat{X}_1))| \leq Ch^3. \tag{23}$$

We first observe that

$$\begin{aligned}\frac{h}{2}(f(K_2) + f(X_0)) &= hf(X_0) + \frac{h^2}{2}\Big(f'(X_0)f(X_0) + \frac{1}{2}\sum_{r=1}^m f''(X_0)(g^r(X_0), g^r(X_0))\Big) \\ &+ \sum_{r=1}^m f'(X_0)(g^r(X_0))\frac{h^{3/2}\xi_r}{2} + h^2R_1 + h^{5/2}R_2 + \mathcal{O}(h^3),\end{aligned}$$

where $R_1 = \frac{1}{4}\sum_{p,q=1}^m f''(X_0)(g^p(X_0), g^q(X_0))(\xi_p\xi_q - \delta_{p,q})$ and $\delta_{p,q}$ is the Kronecker delta function. As $\mathbb{E}(\xi_p\xi_q) = \delta_{r,s}$ we have $\mathbb{E}(R_1) = 0$. Noticing $\mathbb{E}(\xi_p\xi_q\xi_r) = \mathbb{E}(\xi_p) = 0$ for all indices p, q, r, we have also $\mathbb{E}(R_2) = 0$, where

$$R_2 = \frac{1}{2}\sum_{r=1}^m f''(X_0)(g^r(X_0), f(X_0))\xi_r + \frac{1}{12}\sum_{p,q,r=1}^m f'''(X_0)(g^p(X_0), g^q(X_0), g^r(X_0))\xi_p\xi_q\xi_r.$$

Second, a Taylor expansion of the quantity (21) yields

$$\sum_{r=1}^m g^r\Big(\frac{X_0 + K_1}{2}\Big)\sqrt{h}\xi_r + \frac{h^{3/2}}{4}\sum_{q,r=1}^m (g^r)''(X_0)(g^q(X_0), g^q(X_0))\xi_r + h^{3/2}R_3 + h^{5/2}R_4 + \mathcal{O}(h^3),$$

where $R_3 = \frac{1}{4}\sum_{p,q,r=1}^m (g^r)''(X_0)(g^q(X_0), g^p(X_0))(\chi_q\chi_p - \delta_{q,p})\xi_r$ which yields $\mathbb{E}(R_3) = 0$ using $\mathbb{E}((\chi_q\chi_p - \delta_{q,p})\xi_r) = 0$. In addition, using $R_4 = \frac{1}{8}\sum_{p,q,r=1}^m (g^r)'''(X_0)(g^p(X_0), g^q(X_0), f(X_0))\chi_p\chi_q\xi_r$ yields $\mathbb{E}(R_4) = 0$. Third, we see that

$$\sum_{r=1}^m g^r\Big(\frac{X_0 + K_1}{2}\Big)\sqrt{h}\xi_r = \sum_{r=1}^m \Big(\sqrt{h}g^r(X_0) + \frac{1}{2}h^{3/2}(g^r)'(X_0)f(X_0)\Big)\xi_r + h^{5/2}R_5 + \mathcal{O}(h^3), \tag{24}$$

where $R_5 = \frac{1}{8}\sum_{r=1}^m (g^r)''(X_0)(f(X_0), f(X_0))\xi_r$, which yields $\mathbb{E}(R_5) = 0$. Combining these estimates with (20), we obtain

$$\bar{X}_1 - \hat{X}_1 = h^{3/2}R_3 + h^2R_1 + h^{5/2}(R_2 + R_4 + R_5) + \mathcal{O}(h^3). \tag{25}$$

Using $\bar{X}_1 - \hat{X}_1 = \mathcal{O}(h^{3/2})$, a Taylor expansion yields $\phi(\bar{X}_1) - \phi(\hat{X}_1) = \phi'(\hat{X}_1)(\bar{X}_1 - \hat{X}_1) + \mathcal{O}(h^3)$. Setting $G = \sum_{r=1}^m g^r(X_0)\xi_r$, we further Taylor expand the quantity $\phi'(\hat{X}_1)$ and obtain, using (25),

$$\begin{aligned}\phi(\bar{X}_1) - \phi(\hat{X}_1) &= \phi'(X_0 + \sqrt{h}G + hf(X_0) + \mathcal{O}(h^{3/2}))(\bar{X}_1 - \hat{X}_1) + \mathcal{O}(h^3) \\ &= \phi'(X_0)(\bar{X}_1 - \hat{X}_1) + h^2\phi''(X_0)(G, R_3) + h^{5/2}\phi''(X_0)(G, R_1) \\ &+ h^{5/2}\phi''(X_0)(f(X_0), R_3) + \frac{h^{5/2}}{2}\phi'''(X_0)(G, G, R_3) + \mathcal{O}(h^3).\end{aligned}$$

We notice that $\mathbb{E}(\phi'(X_0)(\bar{X}_1 - \hat{X}_1)) = \mathcal{O}(h^3)$ and each of the other above terms have expectancy zero (for the terms involving both G and R_3, we use the independence of the random variables χ_q, ξ_r). This proves the local error estimate (23). To conclude the proof of the global error estimate by using Remark 2.1, it remains to check that for all $r \in \mathbb{N}$ the moments $\mathbb{E}(|X_n|^{2r})$ are bounded uniformly with respect to all h small enough for all $0 \leq nh \leq T$. We use here the approach of [27, Lemma 2.2, p. 102] which states that it is sufficient to show

$$|\mathbb{E}(\bar{X}_{n+1} - \bar{X}_n | \bar{X}_n)| \leq C(1 + |\bar{X}_n|)h, \qquad |\bar{X}_{n+1} - \bar{X}_n| \leq M_n(1 + |\bar{X}_n|)\sqrt{h}, \tag{26}$$

where C is independent of h and M_n is a random variable with moments of all orders bounded uniformly with respect to all h small enough. These estimates are a straightforward consequence of the definition (22) of the scheme and the linear growths of f, g (a consequence of their Lischitzness). □

3.2 Stabilization procedure

All the second order methods considered in this paper (drift implicit or explicit) applied to the linear test problem (12) have a stability function (13) of the form

$$R(p, q, \xi) = A(p) + B(p)q\xi + C(p)\frac{q^2}{2}\left(\xi^2 - 1\right), \tag{27}$$

where ξ is either a Gaussian random variable $\mathcal{N}(0, 1)$ or a three points discrete random variable (16). The numerical mean-square stability domain (14) for methods having the above stability function can be characterized by [15]

$$S_{num}^{MS} = \left\{ (p, q) \in \mathbb{C}^2 \; ; |A(p)|^2 + |B(p)q|^2 + \frac{1}{2}|C(p)q^2|^2 < 1 \right\}, \tag{28}$$

while assuming here a three points discrete random variable is used (see ξ_r in (16)), the numerical asymptotic stability domain can be characterized straightforwardly by the criteria (15) from [15][4],

$$\begin{aligned} S_{num}^{AS} &= \left\{ (p, q) \in \mathbb{C}^2 \; ; 2/3 \, \log|R(p, q, 0)| + 1/6 \, \log|R(p, q, \sqrt{3})| + 1/6 \, \log|R(p, q, -\sqrt{3})| < 1 \right\} \\ &= \left\{ (p, q) \in \mathbb{C}^2 \; ; \left| \left(A(p) + C(p)q^2\right)^2 - 3B^2(p)q^2 \right| \left| A(p) - \tfrac{1}{2}C(p)q^2 \right|^4 < 1 \right\}. \end{aligned} \tag{29}$$

For example, for the weak Milstein-Talay method (18) and its derivative free version (22), we have

$$A(p) = 1 + p + \frac{1}{2}p^2, \quad B(p) = 1 + p, \quad C(p) = 1. \tag{30}$$

Since visualizing the domains of stability for $(p, q) \in \mathbb{C}^2$ is difficult we restrict ourselves to study the case where $(p, q) \in \mathbb{R}^2$. It can be seen in Figure 1 that the weak Milstein-Talay method (18) has restricted mean-square and asymptotic stability regions. This is expected for classical explicit methods and our goal is to introduce a stabilization procedure that permits to enlarge them significantly. We first define for $a > 0$ the following "portion of the true mean-square stability region"

$$\mathcal{S}_a^{MS} = \{(p, q) \in (-a, 0) \times \mathbb{R} \; ; \; p + \frac{1}{2}|q|^2 < 0\}, \tag{31}$$

[4] In (29), we set $\log 0 := -\infty$. Notice that for $\xi \sim \mathcal{N}(0, 1)$ numerical asymptotic stability domains S_{num}^{AS} are more difficult to characterize [15].

Milstein-Talay method, see (30)

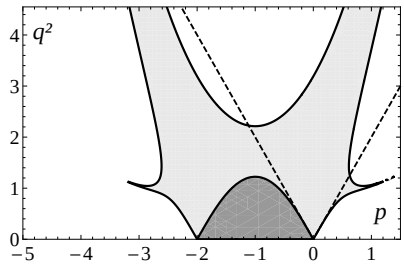

Figure 1: Mean-square stability region (dark gray) and asymptotic stability region (dark and light grays) of the explicit second order Milstein-Talay method with stability function (27).

and define for a given method

$$\ell = \sup\{a > 0 \ ; \ \mathcal{S}_a^{MS} \subset \mathcal{S}_{num}^{MS}\}, \quad d = \sup\{a > 0 \ ; \ (-a, 0) \times \{0\} \subset \mathcal{S}_{num}^{MS}\}, \tag{32}$$

where d is the size of the stability domain along the deterministic p-axis (observe that $d \geq \ell$). For the Milstein-Talay method we have $\ell = 0, d = 2$. In contrast, the S-ROCK2 methods (see (44), Section 3.3) have values ℓ, d increasing quadratically with the stage parameter s. In turn, the ratio of stability versus work increases linearly, while for classical explicit methods it is bounded.

Weak order one S-ROCK methods [4] For ordinary differential equations (ODEs),

$$\frac{dX(t)}{dt} = f(X(t)), \qquad X(0) = X_0, \tag{33}$$

a well-know stabilization procedure for the Euler method has been proposed in [38]. Its construction is based on the classical Chebyshev polynomials $T_s(\cos x) = \cos(sx)$. Given an integer $s \geq 1$, the number of stages, and a damping parameter $\eta \geq 0$, we define the following Runge-Kutta method (first order Chebyshev method) with step size h by the following explicit recursion where

$$\begin{aligned} K_0 &= X_0, \quad K_1 = X_0 + h\frac{\omega_1}{\omega_0} f(K_0), \\ K_j &= 2h\frac{T_{j-1}(\omega_0)}{T_j(\omega_0)} f(K_{j-1}) + 2\omega_0 \frac{T_{j-1}(\omega_0)}{T_j(\omega_0)} K_{j-1} - \frac{T_{j-2}(\omega_0)}{T_j(\omega_0)} K_{j-2}, \quad j = 2, \ldots, s \\ X_1 &= K_s, \end{aligned} \tag{34}$$

$\omega_0 = 1 + \frac{\eta}{s^2}, \quad \omega_1 = \frac{T_s(\omega_0)}{T_s'(\omega_0)}$. Applied to the linear test problem $dX(t)/dt = \lambda X(t)$ the method (34) gives $X_1 = R_s(p)X_0$, where $p = \lambda h$ and where $R_s(p)$, called the stability function (polynomial) of the method, is given by $R_s(p) = T_s(\omega_0 + \omega_1 p)/T_s(\omega_0)$. We emphasize that (34) denotes in fact a family of methods indexed by the stage number s. A crucial property of the methods (34) is

$$|R_s(p)| \leq 1 \ \text{ for all } p \in (-d_s, 0), \tag{35}$$

with $d_s \simeq C \cdot s^2$, for s large enough, where C depends on the damping parameter η (for $\eta = 0$, $C = 2$). Thus, the length d_s of the stability domain

$$\mathcal{S} := \{p \in \mathbb{C}; |R(z)| \leq 1\} \tag{36}$$

of the methods increases quadratically with s on the negative real axis. This quadratic growth of the stability domain is the key feature of such methods compared to standard explicit integrators.

The idea for stabilizing the Euler-Maruyama (7) is now simply to damp its stability function $R(p,q,\xi) = 1+p+q\xi$, obtained by applying (7) to (12) using $R_s(p)$ (with a value of the damping η optimized for each s, see [4]). The corresponding Runge-Kutta type scheme reads [4]

$$\begin{aligned} K_0 &= X_0, \quad K_1 = X_0 + h\frac{\omega_1}{\omega_0} f(K_0), \\ K_j &= 2h\frac{T_{j-1}(\omega_0)}{T_j(\omega_0)} f(K_{j-1}) + 2\omega_0 \frac{T_{j-1}(\omega_0)}{T_j(\omega_0)} K_{j-1} - \frac{T_{j-2}(\omega_0)}{T_j(\omega_0)} K_{j-2}, \quad j = 2,\ldots,s \\ X_1 &= K_s + \sum_{r=1}^{m} g^r(K_s)\Delta W_r. \end{aligned} \tag{37}$$

The method (37) will be denoted by S-ROCK(1/2,1). Another method of strong order 1 and weak order 1 has been considered in [4]. Using the approximation (20) from [31], a multi-dimensional derivative free version, denoted S-ROCK(1,1), can be obtained straightforwardly by replacing the last line in (37) by

$$X_1 = K_s + \sum_{r=1}^{m} g^r(K_s)\Delta W_r + \frac{1}{2}\sum_{r=1}^{m}\Big(g^r\big(K_s + \sum_{q=1}^{m} g^q(K_s) I_{q,r}\big) - g^r\big(K_s - \sum_{q=1}^{m} g^q(K_s) I_{q,r}\big)\Big),$$

where $I_{q,r}$ are defined in (9) and by considering a larger damping η as discussed in [4] (see also the related work [20]). It turns out that S-ROCK(1/2,1) and S-ROCK(1,1) include a portion of the true mean-square stability region that scales like $\ell_s \simeq 0.33 \cdot s^2$ and $\ell_s \simeq 0.19 \cdot s^2$, respectively.

Second order stabilization Similarly as for the weak order one S-ROCK method, the idea is to stabilize the weak second order method (22). We start with a deterministic stabilized second order Chebyshev method. Recall that the derivation of optimal stability functions suitable for the stabilization of second order (deterministic method) is a non trivial task and various strategies have been proposed [21, 38, 5, 1]. We choose here the second order orthogonal Runge-Kutta Chebyshev methods (ROCK2) introduced in [5]. The idea is to search for a stability polynomial

$$R_s(p) = w_2(p) P_{s-2}(p), \tag{38}$$

where $P_{s-2}(p)$ is a member family of polynomials $\{P_j(z)\}_{j\geq 0}$ orthogonal with respect to the weight function $\frac{w_2(x)^2}{\sqrt{1-x^2}}$. The polynomial P_{s-2} has degree $s-2$, while w_2 is a positive polynomial of degree two (depending on s). One constructs the polynomials w_2 such that R_s satisfies [5]

$$R_s(p) = 1 + p + \frac{p^2}{2} + \mathcal{O}(p^3), \tag{39}$$

together with a large stability interval (35), increasing as $\simeq 0.81 \cdot s^2$ along the negative real axis. Thanks to the recurrence relation of the orthogonal polynomials $\{P_j(z)\}_{j\geq 0}$, a method of order two for (33) based on a recurrence formula can be constructed [5]

$$\begin{aligned} K_0 &= X_0, \quad K_1 = K_0 + \mu_1 h f(K_0), \\ K_j &= \mu_j h f(K_{j-1}) - \nu_j K_{j-1} - \kappa_j K_{j-2}, \quad j = 2,\cdots,s-2, \\ K_{s-1} &= K_{s-2} + 2\tau h f(K_{s-2}), \\ X_1 &= K_{s-2} + \left(2\sigma - \frac{1}{2}\right) h f(K_{s-2}) + \frac{1}{2} h f(K_{s-1}). \end{aligned} \tag{40}$$

[5] The two last stages of the method are written is a slightly different way as in the ROCK2 method [5, Equ. (26-27)] as (40) is more convenient for an extension to stochastic integrators. We emphasize that it has the same order and stability properties as the ROCK2 method [5, Equ. (26-27)].

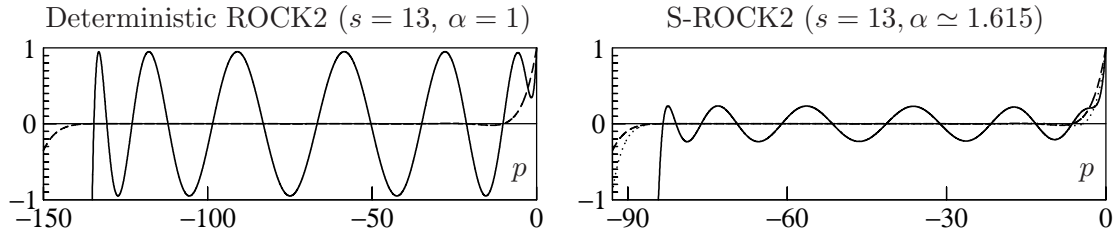

Figure 2: Comparison of polynomials involved in ROCK2 and S-ROCK2 for $s = 13$. Polynomials $R_{s,\alpha}$ (solid lines), $P_{s-2}(\alpha p)$ (dashed lines). We also include the polynomial $P_s(\alpha p)$ in the right picture (dotted lines).

The parameters μ_j, k_j (depending on s) are obtained from the three-term recurrence relation [5, eq. (24)-(25)] of the orthogonal polynomials $\{P_j(z)\}_{j\geq 0}$, while σ, τ (that also depend on s) satisfy $w_2(p) = 1 + 2\sigma p + \tau p^2$ and are chosen such that (39) holds.

In preparation for the extension of the ROCK2 methods to stochastic problems, we now explain a novel strategy to introduce damping in the scheme (40). The idea is to consider the following scheme for a fixed scalar parameter α.

$$\begin{aligned} K_0 &= X_0, \quad K_1 = K_0 + \alpha\mu_1 h f(K_0), \\ K_j &= \alpha\mu_j h f(K_{j-1}) - \nu_j K_{j-1} - \kappa_j K_{j-2}, \quad j = 2, \cdots, s-2, \\ K_{s-1} &= K_{s-2} + 2\tau_\alpha h f(K_{s-2}) \\ X_1 &= K_{s-2} + \left(2\sigma_\alpha - \frac{1}{2}\right) h f(K_{s-2}) + \frac{1}{2} h f(K_{s-1}). \end{aligned} \tag{41}$$

Notice that for $\alpha = 1$, we recover the original ROCK2 method (40). Applied to the linear test problem $dX/dt = \lambda X, X(0) = X_0$ this method yields (setting $p = h\lambda$ and $X_0 = 1$)

$$X_1 = (1 + 2\sigma_\alpha p + \tau_\alpha p^2) P_{s-2}(\alpha p) =: R_{s,\alpha}(p). \tag{42}$$

Lemma 3.2. *The method* (41) *has second order for the system of ODEs* (33) *for any* α *provided*

$$\sigma_\alpha = \frac{1-\alpha}{2} + \alpha\sigma, \quad \tau_\alpha = \frac{(\alpha-1)^2}{2} + 2\alpha(1-\alpha)\sigma + \alpha^2\tau. \tag{43}$$

Proof. Recall that for second order deterministic methods, standard Runge-Kutta order conditions for linear and nonlinear problems are identical. From (39) we deduce the relation $P'_{s-2}(0) = 1 - 2\sigma$ and $\frac{1}{2}P''_{s-2}(0) = \frac{1}{2} - \tau - 2\sigma(1-2\sigma)$. Imposing the second order condition to (42) yields

$$(1 + 2\sigma_\alpha p + \tau_\alpha p^2)(1 + P'_{s-2}(0)\alpha p + \frac{1}{2}P''_{s-2}(0)(\alpha p)^2 + \mathcal{O}(p^3)) = 1 + p + \frac{p^2}{2} + \mathcal{O}(p^3),$$

which is equivalent to the relations (43). □

In Figure 2, we plot, for $s = 13$, the polynomials $P_{s-2}(\alpha p)$ and $R_{s,\alpha}(p)$ (defined in (42)) involved in the standard ROCK2 method ($\alpha = 1$, left picture) and the S-ROCK2 method ($\alpha \simeq 1.615$ right picture) introduced in the next section. It can be seen that increasing α reduces the amplitude of the oscillations of $R_{s,\alpha}(p)$. The appropriate choice of α is discussed below.

3.3 The S-ROCK2 methods

We introduce here our new explicit stabilized integrator, obtained by stabilizing the Milstein-Talay method (22) with (41).

S-ROCK-2 integrator of weak order two Given X_0, compute X_1 as follows.

$$\begin{aligned}
K_0 &= X_0, \quad K_1 = K_0 + \alpha\mu_1 h f(K_0),\\
K_j &= \mu_j \alpha h f(K_{j-1}) - \nu_j K_{j-1} - \kappa_j K_{j-2}, \quad j = 2, \cdots, s,\\
K^*_{s-1} &= K_{s-2} + 2\tau_\alpha h f(K_{s-2}) + \sqrt{h}\sum_{r=1}^{m} g^r(K_s)\xi_r,\\
X_1 &= K_{s-2} + \Big(2\sigma_\alpha - \frac{1}{2}\Big) h f(K_{s-2}) + \frac{1}{2} h f(K^*_{s-1})\\
&+ \frac{1}{2}\sum_{r=1}^{m}\Big(g^r\Big(K_s + \sum_{q=1}^{m} g^q(K_s) J_{q,r}\Big) - g^r\Big(K_s - \sum_{q=1}^{m} g^q(K_s) J_{q,r}\Big)\Big)\\
&+ \frac{\sqrt{h}}{2}\sum_{r=1}^{m}\Big(g^r\big(K_{s-1} + \sqrt{\frac{h}{2}}\sum_{q=1}^{m} g^q(K_s)\chi_q\big) + g^r\big(K_{s-1} - \sqrt{\frac{h}{2}}\sum_{q=1}^{m} g^q(K_s)\chi_q\big)\Big)\xi_r. \quad (44)
\end{aligned}$$

where $\alpha = 1/(2P'_{s-1}(0))$ and $\sigma_\alpha, \tau_\alpha$ are given by (43). Here, the constants $\mu_j, \nu_j, \kappa_j, \sigma, \tau$ depend on s and are the same as for the standard deterministic ROCK2 integrator (40).

integrator	work			stability	
	$\#f$	$\#g^r$	#random	d_s	ℓ_s
s steps of Milstein-Talay (22)	$2s$	$5s$	$2ms$	$2s$	0
one step of S-ROCK2 (44)	$s+2$	5	$2m$	$\simeq 0.42(s+2)^2$	$\simeq 0.42(s+2)^2$

Table 1: Computational complexity for an SDE in dimensions N (drift) and m (diffusion).

Numerical computations show that the S-ROCK2 method includes a portion of the true mean-square stability region $\mathcal{S}^{MS}_\ell$ that grows with the stage number as $\ell_{\text{S-ROCK2}} \simeq 0.42(s+2)^2$. The computational complexity of one step of the S-ROCK2 method with stepsize h is reported in Table 1 and compared to s steps with stepsize h/s of the weak second order Milstein-Talay method (22). As observed, one step of the S-ROCK2 method (44) requires at each step $\#f = s+2$ evaluations of the drift function, $\#g^r = 5$ evaluations of the diffusion functions g^r, $r = 1, \ldots, m$, and $\#random = 2m$ simulations of independent discrete random variables, independently of the dimensions N, m of the considered SDE. The main feature of our S-ROCK2 integrators is that the mean-square stability region sizes ℓ_s, d_s grow quadratically with respect to the computational work $\#f + \#g^r$, while $\ell_s = 0$ and d_s grows only linearly for the standard explicit methods.

Remark 3.3. *(Diagonal noise) When $N = m$ and $(g^1(x), \ldots, g^N(x)) = \mathrm{diag}(g_1(x^1), \ldots, g_N(x^N))$ is a diagonal matrix where $g_k(x)$ depends only on x^k, one can replace the two last lines of* (44) *by $G = \big(G_1, \ldots, G_N\big)^T$ where $G_k = \frac{1}{2}\Big(g_k\big(K_{s,k} + g_k(K_{s,k})J_{k,k}\big) - g_k\big(K_{s,k} - g_k(K_{s,k})J_{k,k}\big)\Big) + \frac{\sqrt{h}}{2}\left(g_k(K_{s-1,k} + \sqrt{\frac{h}{2}}g_k(K_{s,k})) + g_k(K_{s-1,k} - \sqrt{\frac{h}{2}}g_k(K_{s,k}))\right)\xi_k$ for all $k = 1, \ldots, m$.*

We next prove that the method (44) has indeed weak second order.

Theorem 3.4. *Consider the SDE* (1) *with $f, g^r \in C^6_P(\mathbb{R}^N, \mathbb{R}^N)$, Lipschitz continuous. Then the S-ROCK2 method* (44) *for the approximation of* (1) *satisfies*

$$|\mathbb{E}(\phi(X(nh))) - \mathbb{E}(\phi(X_n))| \le Ch^2, \quad 0 \le nh \le T$$

for all $\phi \in C^6_P(\mathbb{R}^N, \mathbb{R})$, where C is independent of n, h.

Proof. Noticing that $K_j = X_0 + \alpha P_j'(0) h f(X_0) + \mathcal{O}(h^2)$ and using Lemma 3.2 yields

$$K_{s-2} + \Big(2\sigma_\alpha - \frac{1}{2}\Big) h f(K_{s-2}) + \frac{1}{2} h f(K_{s-2} + 2\tau_\alpha h f(K_{s-2})) = X_0 + \big(hf + \frac{h^2}{2} f'f\big)(X_0) + \mathcal{O}(h^3).$$

The choice $\alpha = 1/(2P_{s-1}'(0))$ yields $K_{s-1} = X_0 + \frac{h}{2} f(X_0) + \mathcal{O}(h^2)$. We deduce $X_1 - \bar{X}_1 = h^2 R_1 + h^{5/2} R_2 + \mathcal{O}(h^3)$, where $\bar{X}_1$ is defined by the derivative free Milstein-Talay method (22) and

$$\begin{aligned} R_1 &= \alpha P_s'(0) \sum_{q,r=1}^{m} \big((g^r)''(g^q, f) + (g^r)'(g^q)' f\big) J_{q,r} \\ R_2 &= \frac{\alpha P_s'(0)}{2} \sum_{r=1}^{m} f'(g^r)' f \xi_r + \alpha^2 P_{s-1}''(0) \sum_{r=1}^{m} (g^r)' f' f \xi_r \\ &+ \frac{\alpha P_s'(0)}{4} \sum_{p,q,r=1}^{m} \big((g^r)'''(g^p, g^q, f) + 2(g^r)''((g^p)' f, g^q)\big) \chi_p \chi_q \xi_r \end{aligned}$$

where in R_1, R_2 the functions f, g^r and their differentials are evaluated at X_0. Observing $\mathbb{E}(R_1) = \mathbb{E}(R_1 \xi_r) = \mathbb{E}(R_2) = 0$ for all r, we obtain the weak estimate (23) for $X_1, \bar{X}_1$, and we conclude the proof of Theorem 3.4 using Remark 2.1, similarly to the end of the proof of Lemma 3.1. We refer to the proof of [4, Thm. 4.2] for details on deriving the estimates (26) in the context of stochastic stabilized explicit integrators. □

Remark 3.5. *Consider the integrator $\hat{X}_1$ obtained from* (44) *by replacing the ξ_r by independent Gaussian variables, i.e., $\xi_r \sim \mathcal{N}(0,1)$. This integrator has then strong order one in the case of a commutative noise (notice that in this case the left-hand side of* (20) *becomes independent from the values of the χ_r random variables). In the general case of non-commutative noise, if one further replaces the discrete random variables $J_{q,r}$ by the usual multiple stochastic integrals* (9)*, then $\hat{X}_1$ remains of strong order one. Indeed, using Remark 2.1 and owing to the second weak order of* (44) *one only needs to show the first inequality of* (6)*. Furthermore instead of comparing $\hat{X}_1$ to $X(t_1)$ it is sufficient to compare $\hat{X}_1$ to* (8) *as this latter method is known to have strong order one. The remaining calculations are straightforward.*

Stability analysis We now focus on the mean-square and asymptotic stability properties of our new explicit weak second order integrator.

Proposition 3.6. *Consider the S-ROCK2 method* (44) *applied to the linear test equation* (12)*. The numerical asymptotic stability domain S_{num}^{AS} defined in* (15) *is given by* (29) *and the numerical mean-square stability domain S_{num}^{MS} defined in* (14) *is given by* (28) *where the polynomial functions $A(p), B(p), C(p)$ are defined by*

$$A(p) = P_{s-2}(\alpha p)(1 + 2\sigma_\alpha p + \tau_\alpha p^2), \quad B(p) = P_{s-1}(\alpha p) + \frac{p}{2} P_s(\alpha p), \quad C(p) = P_s(\alpha p). \tag{45}$$

Proof. Follows from noticing that applied to the linear test problem (12), the method (44) yields (27) with $A(p), B(p), C(p)$ given by (45). □

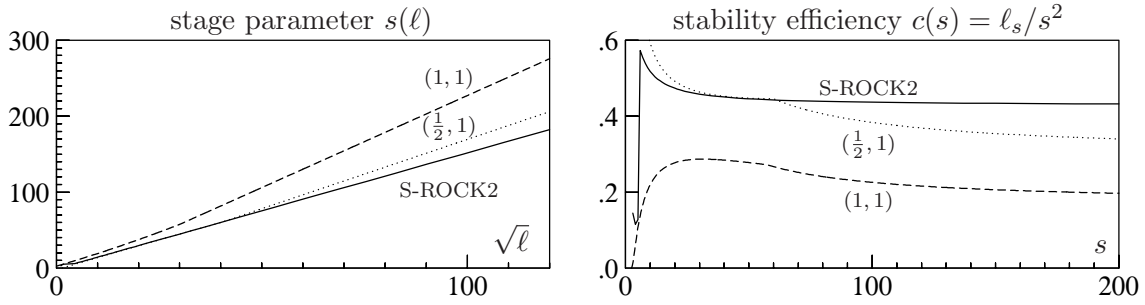

Figure 3: Comparison of S-ROCK2 (solid lines) and the weak order one S-ROCK methods $(1,1)$ (dashed lines), $(\frac{1}{2},1)$ (dotted lines). Left picture: optimal stage parameter s as a function of $\sqrt{\ell}$, where ℓ is given by (32). Right picture: stability efficiency $c(s) = \ell_s/s^2$.

In Figure 4 we plot asymptotic (light gray) and mean-square (dark gray) stability regions for different values of the stage number s. In all cases, we observe the inclusions $\mathcal{S}^{MS}_{num} \cap \mathbb{R}^2 \subset \mathcal{S}^{AS}_{num} \cap \mathbb{R}^2$. The dotted lines where $p < 0$ correspond to the boundary of the true mean-square stability region, while the dotted lines where $p > 0$ (see bottom pictures) correspond to the boundary of the true asymptotic stability region (given by $p + |q|^2/2 = 0$ and $p - q^2/2 = 0$, respectively). In the bottom pictures we zoom close to the origin and observe that the asymptotic stability region contains the mean square stability region. Furthermore, a large portion of the true asymptotic stability region is included in the numerical one close to the origin, $\{(p,q) \in \mathbb{R}^2 \ ; \ |p| \leq 1, |p| < |q| < 2.7\} \subset \mathcal{S}^{AS}_{num}$.

We briefly comment the ideas behind the definition of the scheme (44) that allow favorable mean-square stability properties. Recall that the deterministic stability functions $A(p)$ oscillates around the negative real axis (see top left picture in Figure 2). If the absolute value of the local maxima and minima of $A(p)$ are close to one, then in view of (28) we will have gaps in the mean-square stability domains (in the regions where $A(p)$ is bounded). We therefore have to damp this term by introducing and tuning the value of α as explained before in Section 3.2. Next it can be observed that the polynomials $P_{s-2}(p), P_{s-1}(p), P_s(p)$ oscillates around zero with a small amplitude of size $\mathcal{O}(p^{-2})$ along the real axis. These polynomials are thus good candidates to damp the Milstein term which corresponds to the q^2 term in the stability function (27). However, simply working with the polynomials $P_{s-2}(p)$ leaves a gap in the mean-square stability regions close to the origin near to the extrema of $P_{s-2}(p)$. For this reason, we consider instead the polynomial $P_s(p)$ to damp the Milstein term which has the advantage that $P'_s(0) > P'_{s-2}(0)$ (faster decay near the origin). The additional advantage of considering simultaneously the three polynomials P_{s-2}, P_{s-1}, and P_s is that their extrema close to the origin do not coincide. This permits to avoid a gap in the mean-square stability domain close to the origin. The polynomials P_{s-1}, P_s (corresponding to the internal stages K_{s-1}, K_s in (44)) are obtained by computing two additional stages compared to the deterministic ROCK2 (41) method.

3.4 Comparison with other stiff integrators

Comparison with S-ROCK method In Figure 3 we plot the length ℓ defined in (32) of the portion of the true mean-square stability region $\mathcal{S}^{MS}_{\ell}$ as a function of the number of stages used. As we can see the behaviour of the S-ROCK2 method is $\ell \simeq Cs^2$ similarly to the S-ROCK methods of weak order 1 discussed in Section 3.2. Furthermore, once can also see that the S-ROCK2 method is actually more efficient from a stability point of view, since the stability efficiency factor $c(s) = \ell_s/s^2$ converges numerically to about 0.42 for large s, which is larger than the S-ROCK(1/2,1/2) and S-ROCK(1,1) values of 0.33 and 0.19, respectively.

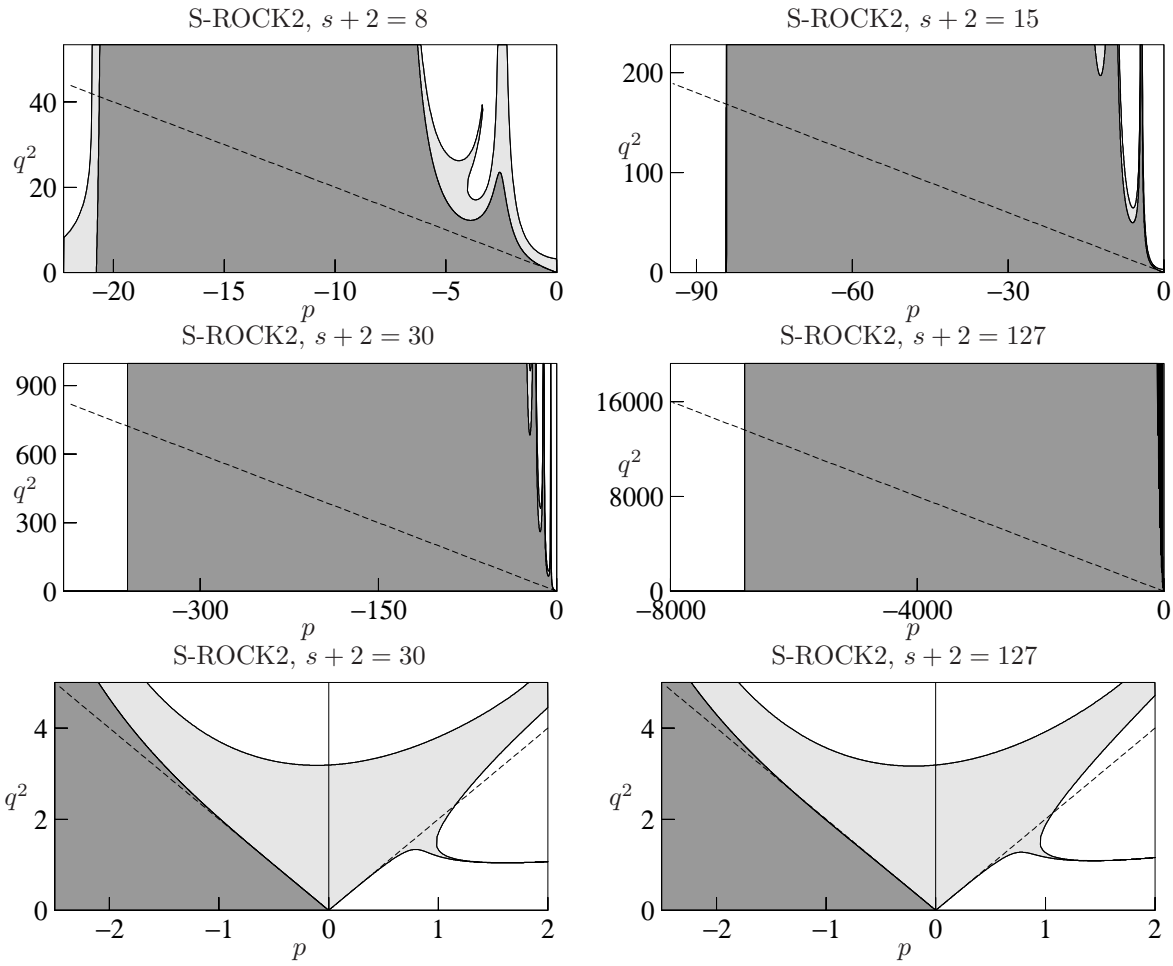

Figure 4: Mean-square stability regions (dark gray) and asymptotic stability regions (dark and light grays) of S-ROCK2 for $s+2=8, 15, 30$, and 127 stages, respectively.

Comparison with a class of diagonally drift-implicit Runge-Kutta methods [11] We have already discussed the asymptotic and mean-square stability properties of the Milstein-Talay method (22), which has restricted mean-square and asymptotic stability regions (see Figure 1). We next consider the weak second-order diagonally implicit Runge-Kutta method (DDIRDI5) derived in [11] with the following aims: reducing the computational cost of a fully drift-implicit method such as the modified θ-Milstein method [3], and improving the stability domains compared to explicit methods. For these method we have (see Fig. 5 for an example with $c_1 = c_2 = 1$)

$$A(p) = 1 + p\frac{1 + (1/2 - c_1 - c_2)p}{(1 - c_1 p)(1 - c_2 p)}, \quad B(p) = 1 + p\frac{1 - (c_1 + c_2)p/2}{(1 - c_1 p)(1 - c_2 p)}, \quad C(p) = 1. \tag{46}$$

Even though the mean-square stability domain has been improved close to the deterministic p axis, it can be seen that this method does not cover a portion of the true mean square stability region. Here as for the explicit Milstein-Talay method, we have $\ell = 0$. This can be seen in Figure 5, where $\mathcal{S}^{MS}_{num} \cap \mathbb{R}^2$ (dark gray) is strictly contained below the curve $p + \frac{1}{2}|q|^2 = 0$ (see dashed lines), which is the boundary of the true mean-square stability region. In fact, the proposition below shows that $\ell = 0$ for the whole class of integrators satisfying (46). Notice however that its deterministic stability domain size defined in (32) is $d = \infty$ in particular for $c_1 = c_2 \geq 1/4$, a feature shared by all reasonable implicit integrators for stiff ODEs.

Proposition 3.7. *Consider a weak order two integrator with a stability function of the form* (27)

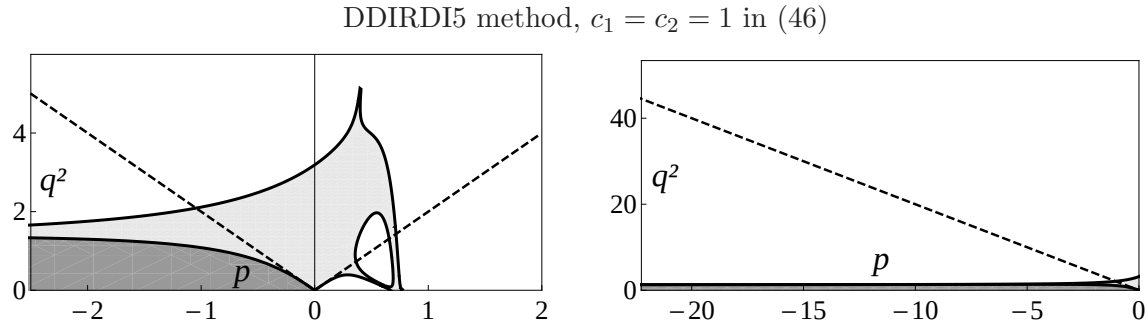

Figure 5: Mean-square stability region (dark gray) and asymptotic stability region (dark and light grays) of the implicit DDIRDI5 with stability function (27) given by (46) (compare with Fig. 4).

when applied to the linear test equation (12)*. A necessary condition for* $\ell \neq 0$ *in* (32) *is*

$$1 + 2B''(0) - 4C'(0) \leq 0. \tag{47}$$

In particular, for the class of integrators with stability function given by (46)*, we have* $\ell = 0$ *for all* $c_1, c_2 \geq 0$*.*

Proof. Using that $\mathbb{E}|R(p,q,\xi)|^2$ can be written as an increasing function of q^2 (see (28)), we have

$$\sup_{(p,q)\in\mathcal{S}_\ell^{MS}} \mathbb{E}(|R(p,q,\xi)|^2) = \sup_{p\in(-\ell,0)} \mathbb{E}(|R(p,\sqrt{-2p},\xi)|^2).$$

Using the weak order two assumption, we have $A(p) = 1+p+p^2/2+\mathcal{O}(p^3)$ and $B(p) = 1+p+\mathcal{O}(p^2)$, a Taylor expansion yields $\mathbb{E}(|R(p,\sqrt{-2p},\xi)|^2) = 1 + (4C'(0) - 2B''(0) - 1)p^3 + \mathcal{O}(p^4)$ which is smaller than 1 for small $-p > 0$ only if (47) holds. For the class of integrators (46), we have $1 + 2B''(0) - 4C'(0) = 1 + 2(c_1 + c_2) > 0$, so the condition (46) is violated. □

Remark 3.8. *Notice that if* $C(p) = 1$*, then the numerical mean-square stability domain is bounded in the* q *direction by* $|q|^4/2 < 1$*. This can be observed in Figure 5 where the mean-square stability region* $\mathcal{S}_{num}^{MS} \cap \mathbb{R}^2$ *(dark gray) of the DDIRDI5 method is bounded vertically by* $|q|^2 < \sqrt{2}$*.*

Comparison with a family of weak second order explicit integrators [19] A family of explicit stabilized integrators for stiff Stratonovitch systems of SDEs has been introduced recently in [19]. Although the stability domain of these methods grows quadratically along the p-axis, with $d_s \simeq 0.54s^2$ (according to the left pictures in [19, Fig. 3]), it can be observed that the mean-square stability domain contains uncontrolled gaps for $|q|^2 > \sqrt{2}$ and we thus have $\ell_s \leq \sqrt{2}$ for all stage parameter s. This makes the algorithm in [19] robust with respect to mean-square stability only in the case of small noises.

4 Numerical experiments

We now present various different numerical experiments with our newly constructed methods. In Section 4.1 we confirm the order of weak convergence of the S-ROCK2 method on two different non-linear problems. Then, in Section 4.2, we test the performance of the S-ROCK2 method for a non-linear stiff problem and compare it to other weak second order methods, while in Section 4.3 we present numerical results for a stochastic PDE arising from Neurosciences.

4.1 Weak convergence rates

We start our numerical investigations by considering two non-stiff non-linear SDEs. The first one is

$$dX(t) = \left(\frac{1}{4}X(t) + \frac{1}{2}\sqrt{X(t)^2+1}\right)dt + \sqrt{\frac{X(t)^2+1}{2}}dW(t), \quad X(0) = 0. \tag{48}$$

The exact solution is $X(t) = \sinh(t/2 + W(t)/\sqrt{2})$, it satisfies $\mathbb{E}\big((\operatorname{arcsinh} X(t))^2\big) = t^2/4 + t/2$.

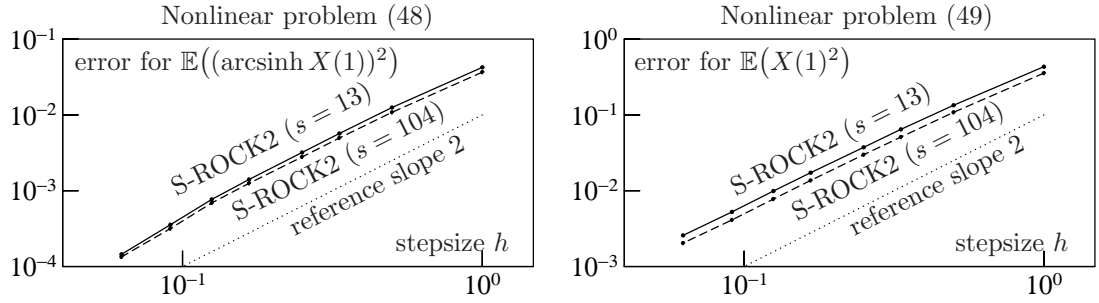

Figure 6: S-ROCK2 method with $s = 13$ stages (solid lines) and $s = 104$ (dashed lines). Weak error at final time $T = 1$ versus the stepsize h for problems (48), (49), where $1/h = 1, 2, 3, 4, 6, 8, 11, 16$.

The second test problem is another nonlinear SDE [11] with 10 independent driving Weiner processes,

$$dX(t) = X(t)dt + \sum_{j=1}^{10} a_j^{-1}\sqrt{X(t) + b_j^{-1}}dW_j(t), \qquad X(0) = 1,$$

with non-commutative noise, where the values of the constants $a_j, j = 1, \ldots, 10$ are respectively $10, 15, 20, 25, 40, 25, 20, 15, 20, 25$, and the values of $b_j, j = 1, \ldots, 10$ are respectively $2, 4, 5, 10, 20$, $2, 4, 5, 10, 20$. For this problem by applying Itô's formula to $\phi(x) = x^2$, taking expectations and using the fact that $\mathbb{E}(X(t)) = e^t$, one calculates

$$\mathbb{E}(X^2(t)) = (-68013 - 458120e^t + 14926133e^{2t})/14400000. \tag{49}$$

We apply the S-ROCK2 method to both problems (48) and (49) and approximate respectively $\mathbb{E}\left((\operatorname{arcsinh} X(T))^2\right)$ and $\mathbb{E}(X^2(T))$ up to the final time $T = 1$ using 10^9 realisations and different step sizes h. We plot the results in Figure 6 and observe that the S-ROCK2 method converges with weak second order for both problems, which confirms the statement of Theorem 3.4. We plot the results for $s = 13$ (solid lines) and $s = 104$ stages (dashed lines) using the same set of generated random numbers. The fact that the obtained curves are nearly identical illustrates that the error constants of the S-ROCK2 methods are nearly independent of the stage number of the integrator, similarly to the standard deterministic ROCK2 integrator (40).

4.2 A nonlinear stiff problem

To illustrate the advantage of including a whole "portion" of the mean-square stability region of the linear test problem (12) we consider the following nonlinear scalar problem with a one-dimensional noise,

$$dX(t) = -\lambda X(t)(1 - X(t))dt - \mu X(t)(1 - X(t))dW(t), \qquad X(0) = 0.95, \tag{50}$$

on time interval $(0, T)$ of length $T = 10$, which is derived from a population dynamics model [12, Chap. 6.2] (see also [4, Example 5.2]). Notice that if one linearizes this problem close to

		parameters: $\varepsilon = 10^{-3}, \lambda = -4$		
method	stepsize	work	$\mathbb{E}(X(1)^2) - 1$	$\mathbb{E}(\lvert X(1)\rvert) - 1$
Milstein-Talay	$h = 1/25$	$\#f = 500, \#g = 1250$	∞ (unstable)	∞ (unstable)
Milstein-Talay	$h = 1/30$	$\#f = 600, \#g = 1500$	-1.1e-2 (stable)	-1.1e-2 (stable)
S-ROCK2($s = 5$)	$h = 1/4$	$\#f = 280, \#g = 200$	3.3e-7 (stable)	1.7e-7 (stable)
		parameters: $\varepsilon = 1, \lambda = -10^2$		
method	stepsize	work	$\mathbb{E}(X(1)^2) - 1$	$\mathbb{E}(\lvert X(1)\rvert) - 1$
Milstein-Talay	$h = 1/280$	$\#f = 5600, \#g = 14000$	∞ (unstable)	∞ (unstable)
Milstein-Talay	$h = 1/300$	$\#f = 6000, \#g = 15000$	0.e0 (stable)	0.e0 (stable)
S-ROCK2($s = 8$)	$h = 1/4$	$\#f = 400, \#g = 200$	0.e0 (stable)	0.e0 (stable)
		parameters: $\varepsilon = 1, \lambda = -10^3$		
method	stepsize	work	$\mathbb{E}(X(1)^2) - 1$	$\mathbb{E}(\lvert X(1)\rvert) - 1$
Milstein-Talay	$h = 1/2800$	$\#f = 56000, \#g = 140000$	∞ (unstable)	∞ (unstable)
Milstein-Talay	$h = 1/3000$	$\#f = 60000, \#g = 150000$	0.e0 (stable)	0.e0 (stable)
S-ROCK2($s = 23$)	$h = 1/4$	$\#f = 1000, \#g = 200$	-3.7e-12 (stable)	-1.8e-12 (stable)

Table 2: Stability efficiency. Work versus stiffness for the second order Milstein-Talay method (22) and the S-ROCK2 methods applied to the nonlinear SDE (50). Averages over 10^6 samples.

the steady solution $X(t) = 1$, it yields the linear test problem (12). Here, the initial condition $X(0) = 0.95$ is chosen close to this stationary solution. We consider the parameters $\lambda < 0, \mu = \sqrt{-\lambda(2-\varepsilon)}$ for which the linear test problem (12) is asymptotic and mean-square stable because $\lambda + |\mu|^2/2 = -\varepsilon/2 < 0$. Recall that for this linear test problem, the S-ROCK2 method is mean-square stable provided $|\lambda|h < \ell_s$, as studied in Section 3.3, while the Milstein-Talay method (18) or (22) is mean-square stable only if h is small enough. We consider two cases.

1. **Case $\varepsilon \ll 1$** We consider first the case where $\lambda < 0$ is a constant of moderate size, e.g. $\lambda = -4$, while $\varepsilon > 0$ is small. Considering the linear test equation (12), the S-ROCK2 method is stable provided $h|\lambda| < \ell_s$, and the stepsize $h = 1/4$ can be used independently of the smallness of ε. In contrast, for the weak second order Milstein-Talay method, a calculation shows that the mean-square stability condition becomes $h|\lambda| \leq \varepsilon/4 + \mathcal{O}(\varepsilon^2)$, and the number of steps needed for a stable integration grows like $\mathcal{O}(4\lambda\varepsilon^{-1})$ as $\varepsilon \to 0$.

2. **Case $|\lambda| \gg 1$** We next consider the case where $\varepsilon = 1$ and $|\lambda| \gg 1$. The S-ROCK method is stable provided $h|\lambda| < \ell_s \simeq Cs^2$ and the minimal number of steps needed for a stable integration grows like $\mathcal{O}(\sqrt{|\lambda|})$ as $\lambda \to \infty$. In contrast, for the weak second order Milstein-Talay method, a calculation yields the mean-square stability condition $h|\lambda| \leq 2$, and the number of steps of the method for a stable integration grows like $\mathcal{O}(|\lambda|)$ as $\lambda \to -\infty$.

We observe in Table 2 the spectacular improvement of the efficiency when switching from the weak second order Milstein-Talay method (22) to the S-ROCK2 methods applied to the nonlinear SDE (50). Indeed, considering three different sets of parameters λ, ε, we observe in all cases that the S-ROCK2 allows one to use a much larger timestep that for the Milstein-Talay method. This significantly reduces the computational cost of each sample, measured in terms of the number of evaluations of the drift and the noise (see $\#f, \#g^r$). We highlight that for the considered parameters ε, λ a sever step size restrictions similar to the explicit Milstein-Talay method would be obtained for the drift-implicit integrators DDIRDI5 of [11] as discussed in Section 3.4, because their mean-square stability domain is bounded on the q axis by $|q|^2 \leq \sqrt{2}$ (see Rem. 3.8 and Fig. 5).

4.3 Electric potential in a neuron

Although our analysis applies only to systems of SDEs, we consider here an SPDE model for the propagation of an electric potential $V(x,t)$ in a neuron [39]. This potential is governed by a system

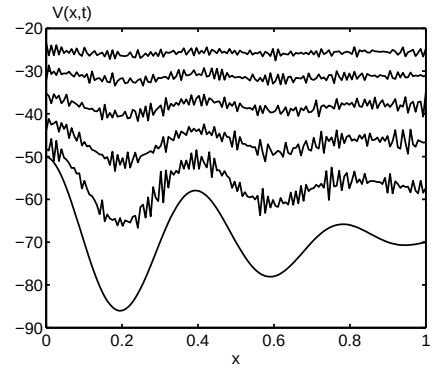

(a) $\Delta t = 1/50$, $\Delta x = 1/150$, fixed t.

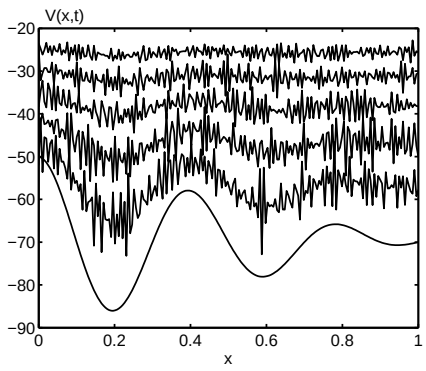

(b) $\Delta t = 1/50$, $\Delta x = 1/200$, fixed t.

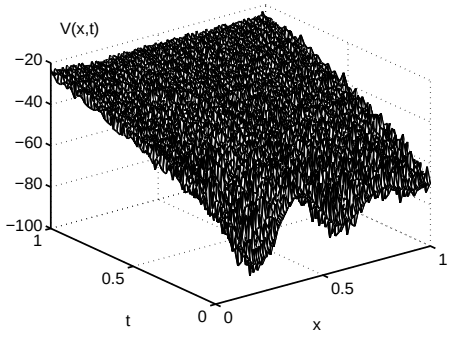

(c) $\Delta t = 1/50$, $\Delta x = 1/200$. Solution $V(x,t)$ as a function of x, t.

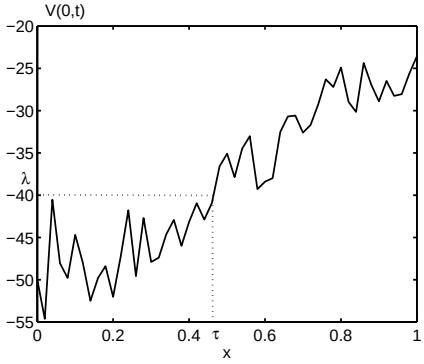

(d) $\Delta t = 1/50$, $\Delta x = 1/200$, fixed $x = 0$.

Figure 7: Samples of realisations of the SPDE (51) (discretized in space) using S-ROCK2 with $s + 2 = 8$ stages (resp. 11) for $\Delta x = 1/150$ (resp. $\Delta x = 1/200$). Figures (a),(b): solutions as functions of x at fixed times $t = 0, 0.2, 0.4, \ldots, 1.0$ (increasing with time, from bottom to top). Figure (d): solution as a function of t for $x = 0$.

of non-linear PDEs called the Hodgkin-Huxley equations [16], but in certain ranges of values of V, this system of PDEs can be well approximated by the cable equation [39].In particular, if the neuron is subject to a uniform input current density over the dendrites and if certain geometric constraints are satisfied, then the electric potential satisfies the following linear cable equation with uniform input current density.

$$\begin{aligned} \frac{\partial V}{\partial t}(x,t) &= \nu \frac{\partial^2 V}{\partial x^2}(x,t) - \beta V(x,t) + \sigma(V(x,t) + V_0)\dot{W}(x,t), \quad 0 \le x, t \le 1, \\ \frac{\partial V}{\partial x}(0,t) &= \frac{\partial V}{\partial x}(1,t) = 0, \quad t > 0, \quad V(x,0) = V_0(x), \quad 0 \le x \le 1, \end{aligned} \tag{51}$$

where $\dot{W}(x,t) = \frac{\partial^2}{\partial x \partial t} w(x,t)$ is a space-time white noise meant in the Itô sense. Here we have assumed that the distance between the origin (or soma) to the dendritic terminals is 1, and that the soma is located at $x = 0$. Furthermore, the white noise term is describing the effect of the arrival of random impulses and the multiplicative noise structure depicts the fact that the response of the neuron to a current impulse may depend on a local potential [39]. The quantity of interest is the threshold time

$$\tau = \inf\{t > 0; V(t,0) > \lambda\}, \tag{52}$$

since when the potential at the soma (somatic depolarization) exceeds the threshold λ the neuron fires an action potential.

The SPDE (51) yields, after space discretization with finite differences [10] the following stiff system of SDE where $V(x_i,t) \approx u_i$, with $x_i = i\Delta x$, $\Delta x = 1/N$,

$$du_i \;=\; \nu\frac{u_{i+1}-2u_i+u_{i-1}}{\Delta x^2}dt - \beta u_i dt + \sigma\frac{u_i+V_0}{\sqrt{\Delta x}}dw_i, \quad i=0,\ldots,N, \tag{53}$$

where the Neumann condition imposes $u_{-1} = u_1$ and $u_{N+1} = u_{N-1}$. Here $w_0, \ldots w_N$ are independent standard Weiner processes, and dw_i indicates Itô noise. We consider the initial condition $V_0(x) = -70 + 20\cos(5\pi x)(1-x)$ and the constants $\nu = 10^{-2}$, $\sigma = 4\cdot 10^{-3}$, $\beta = 1$, $V_0 = 10$, $\lambda = -40$. We consider the time interval $(0,T)$ with $T = 1$. Notice that the noise in (53) is in diagonal form, so we can apply Remark 3.3. We now plot the empirical histograms for the threshold time τ calculated over 10^7 realisations of (53).

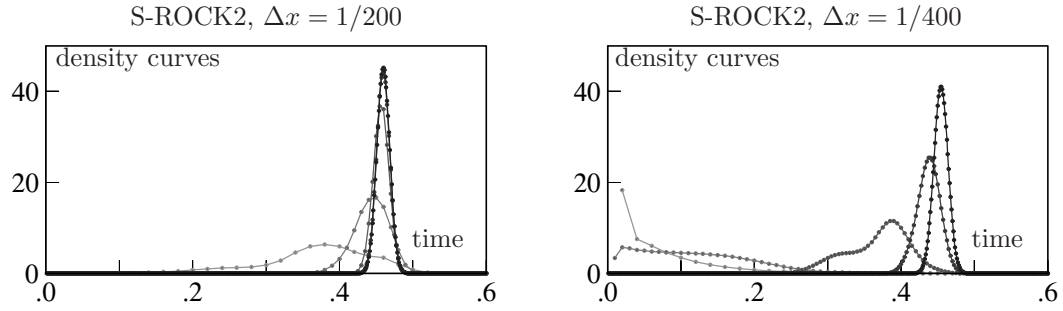

Figure 8: Density plots of the threshold time (52) in the SPDE (51) for various space mesh sizes $\Delta x = 1/200, 1/400$. The four curves in each plot correspond respectively to $\Delta t = 1/50, 1/100, 1/200, 1/400, 1/800$ (light to dark gray).

5 Conclusion

In this paper, we introduced a new family of weak second order explicit stabilized methods, called S-ROCK2, well suited for the integration of stochastic stiff problems. These methods with extended stability regions are shown to be more efficient than standard explicit second order solvers for stiff (mean-square stable) problems, and more efficient than a class of diagonally implicit methods introduced in [11]. The main idea behind the derivation of these methods is to express the S-ROCK2 integrator as a perturbation of the standard Milstein-Talay method. In [6], we show how these ideas can be applied to construct, to the best of our knowledge, the first diagonally drift implicit mean-square A-stable method of weak second order.

Acknowledgements. The authors are grateful to Arnaud Debussche for helpful discussions. The research of A. A. is partially supported by Swiss National Foundation Grant 200021_140692. K.C.Z. was partially supported by Award No. KUK-C1-013-04 of the King Abdullah University of Science and Technology (KAUST).

References

[1] A. Abdulle. Fourth order Chebyshev methods with recurrence relation. *SIAM J. Sci. Comput.*, 23(6):2041–2054, 2002.

[2] A. Abdulle and S. Cirilli. S-ROCK: Chebyshev methods for stiff stochastic differential equations. *SIAM J. Sci. Comput.*, 30(2):997–1014, 2008.

[3] A. Abdulle, D. Cohen, G. Vilmart, and K. C. Zygalakis. High order weak methods for stochastic differential equations based on modified equations. *SIAM J. Sci. Comput.*, 34(3):1800–1823, 2012.

[4] A. Abdulle and T. Li. S-ROCK methods for stiff Ito SDEs. *Commun. Math. Sci.*, 6(4):845–868, 2008.

[5] A. Abdulle and A. Medovikov. Second order Chebyshev methods based on orthogonal polynomials. *Numer. Math.*, 90(1):1–18, 2001.

[6] A. Abdulle, G. Vilmart, and K. C. Zygalakis. Mean-square A-stable diagonally drift-implicit integrators with high order for stiff Ito systems of stochastic differential equations with noncommutative noise. *preprint*, 2012.

[7] L. Arnold. *Stochastic differential equations: theory and applications*. John Wiley and Sons, New york, 1974.

[8] E. Buckwar and C. Kelly. Towards a systematic linear stability analysis of numerical methods for systems of stochastic differential equations. *SIAM Journal on Numerical Analysis*, 48(1):298–321, 2010.

[9] K. Burrage, P. Burrage, and T. Tian. Numerical methods for strong solutions of stochastic differential equations: an overview. *Proc. R. Soc. Lond. Ser. A Math. Phys. Eng. Sci.*, 460(2041):373–402, 2004.

[10] A. M. Davie and J. G. Gaines. Convergence of numerical schemes for the solution of parabolic stochastic partial differential equations. *Math. Comp.*, 70:121–134, 2000.

[11] K. Debrabant and A. Rößler. Diagonally drift-implicit runge–kutta methods of weak order one and two for itô sdes and stability analysis. *Appl. Num. Math.*, 59(3–4):595 – 607, 2009.

[12] T. Gard. *Introduction to stochastic differential equations*. Marcel Dekker, New York, 1988.

[13] E. Hairer and G. Wanner. *Solving ordinary differential equations II. Stiff and differential-algebraic problems*. Springer-Verlag, Berlin and Heidelberg, 1996.

[14] R. Hasminskii. *Stochastic stability of differential equations*. Sijthoff and Noordhoff, The Netherlands, 1980.

[15] D. Higham. A-stability and stochastic mean-square stability. *BIT*, 40:404–409, 2000.

[16] A. L. Hodgkin and A. F. Huxley. A quantitative description of membrane current and its application to conduction and excitation in nerve. *J. of Physiology*, 117(4):500–544, 1952.

[17] P. Kloeden and E. Platen. *Numerical solution of stochastic differential equations*. Springer-Verlag, Berlin and New York, 1992.

[18] P. Kloeden, E. Platen, and N. Hofmann. Extrapolation methods for the weak approximation of Itô diffusions. *SIAM J. Numer. Anal.*, 32(5):1519–1534, 1995.

[19] Y. Komori and K. Burrage. Weak second order S-ROCK methods for stratonovich stochastic differential equations. *J. Comput. Appl. Math.*, 236(11):2895 – 2908, 2012.

[20] Y. Komori and K. Burrage. Strong first order S-ROCK methods for stochastic differential equations. *Comput. Appl. Math.*, 242:261–274, 2013.

[21] V. Lebedev. Explicit difference schemes with time-variable steps for solving stiff systems of equations. *Sov. J. Numer. Anal. Math. Modelling*, 4(2):111–135, 1989.

[22] X. Mao. Stochastic stabilization and destabilization. *Systems Control Lett.*, 23(4):279–290, 1994.

[23] G. Maruyama. Continuous markov processes and stochastic equations. *Rend. Circ. Mat. Palermo*, 4:48–90, 1955.

[24] G. N. Milstein. A method of second order accuracy integration of stochastic differential equation. *Theory Probab. Appl.*, 23:396–401, 1978.

[25] G. N. Milstein. Weak approximation of solutions of systems of stochastic differential equations. *Theory Probab. Appl.*, 30(4):750–766, 1986.

[26] G. N. Milstein. A theorem on the order of convergence of mean-square approximations of solutions of systems of stochastic differential equations. *Teor. Veroyatnost. i Primenen.*, 32(4):809–811, 1987.

[27] G. N. Milstein and M. V. Tretyakov. *Stochastic numerics for Mathematical Physics*. Scientific Computing. Springer-Verlag, Berlin and New York, 2004.

[28] E. Platen. High-order weak approximation of ito diffusions by markov chains. *Probab. Engrg. Inform. Sci.*, 6:391–408, 1992.

[29] A. Rathinasamy and K. Balachandran. Mean-square stability of second-order Runge-Kutta methods for multi-dimensional linear stochastic differential systems. *J. Comput. Appl. Math.*, 219(1):170–197, 2008.

[30] A. Rößler. *Runge-Kutta methods for the numerical solution of stochastic diifferential equations*. Diss. TU Darmstadt. Shaker Verlag, Aachen, 2003.

[31] A. Rößler. Second order Runge-Kutta methods for Itô stochastic differential equations. *SIAM J. Numer. Anal.*, 47(3):1713–1738, 2009.

[32] Y. Saito and T. Mitsui. Stability analysis of numerical schemes for stochastic differential equations. *SIAM J. Numer. Anal.*, 33:2254–2267, 1996.

[33] Y. Saito and T. Mitsui. Mean-square stability of numerical schemes for stochastic differential systems. *Vietnam J. Math.*, 30(suppl.):551–560, 2002.

[34] D. Talay. Efficient numerical schemes for the approximation of expectations of functionals of the solution of a SDE and applications. *Lecture Notes in Control and Inform. Sci., Springer*, 61:294–313, 1984.

[35] D. Talay and L. Tubaro. Expansion of the global error for numerical schemes solving stochastic differential equations. *Stochastic Anal. Appl.*, 8(4):483–509 (1991), 1990.

[36] A. Tocino. Mean-square stability of second-order Runge-Kutta methods for stochastic differential equations. *J. Comput. Appl. Math.*, 175(2):355–367, 2005.

[37] A. Tocino and J. Vigo-Aguiar. Weak second order conditions for stochastic Runge-Kutta methods. *SIAM J. Sci. Comput.*, 24(2):507–523, 2002.

[38] P. Van der Houwen and B. Sommeijer. On the internal stage Runge-Kutta methods for large m-values. *Z. Angew. Math. Mech.*, 60:479–485, 1980.

[39] J. Walsh. An introduction to stochastic partial differential equations. In P. L. Hennequin, editor, *École d'Été de Probabilités de Saint Flour XIV - 1984*, volume 1180 of *Lecture Notes in Mathematics*, chapter 3, pages 265–439. Springer Berlin / Heidelberg, 1986.